18TH WORLD CONFERENCE ON EARTHQUAKE ENGINEERING
WCEE2024
MILAN

MILAN, ITALY
30TH JUNE - 5TH JULY 2024
www.wcee2024.it

DAMPING PERFORMANCE EVALUATION OF A SEMI-ACTIVE CONTROLLED BASE-ISOLATION SYSTEM BY ARX MODEL

Y. Sugiyama[1], M. Hashimoto[2], H. Fujitani[2] & Y. Mukai[2]

[1] Kobe University, Kobe City, Japan, 239t026t@stu.kobe-u.ac.jp

[2] Kobe University, Kobe City, Japan

Abstract: *The application of semi-active control is expected to reduce the response displacement of a base-isolation layer effectively without increasing the floor response acceleration of a superstructure under near-fault pulse ground motion and long-period ground motion. Although some studies have evaluated response reduction effects achieved using a common parameter in passive control, few studies have examined the response reduction effects obtained using a physical value in semi-active control. Therefore, for this study, the response reduction effects of semi-active control systems were evaluated using the damping factor based on the ARX model. The ARX model is a time-domain system identification method that can identify the natural frequency and the damping factor of the target structure using ground acceleration as input data and absolute acceleration of the structure as output data. First, real-time hybrid simulation (RTHS) of a semi-active base-isolation system with an installed magnetorheological fluid damper (MR damper) was conducted to verify the effectiveness of semi-active control under near-fault pulse ground motion and long-period ground motion. The effectiveness of the evaluation method using RTHS has been validated through comparison with large-scale shaking table tests conducted at E-defense. The results obtained for RTHS confirmed that semi-active control exhibits high acceleration reduction effects for some ground motions. Particularly, sliding mode control (SMC) was able to reduce the absolute acceleration significantly more than passive control. Additionally, the damping factor based on the ARX model enabled the evaluation of differences in control effects among several control algorithms. Results demonstrated the possibility of expressing the response reduction effects of each control algorithm using a common physical parameter: the damping factor.*

1. Introduction

In recent years, the occurrence of large-amplitude seismic motions has become a concern. They have become a social issue that must be addressed to ensure not only structural safety but also the continuous usability of buildings. A base-isolation system semi-actively controlled using an MR damper is regarded as an effective means of addressing this issue, for example, Johnson et al. (1998), Fujii et al. (2007). In fact, a semi-active base-isolation system can reduce the response displacement of the isolation layer effectively without increasing the floor response acceleration of the superstructure. Although some studies have evaluated response reduction effects using a common parameter in passive control, few studies have examined the response reduction effects using a physical value in semi-active control. For this study, RTHS reproduces the response of a base-isolated single-degree-of-freedom system controlled semi-actively with an MR damper. The ARX model, a system identification method, is applied to the obtained RTHS results for quantitative evaluation of the effects of passive control and semi-active control by the damping factor.

2. Outline of the shaking table test

2.1. Real-Time Hybrid Simulation (RTHS) (Itahara et al. (2020))

The model used for experimentation is a base-isolated single-degree-of-freedom system with an MR damper. The model is shown in Figure 1. The model parameters are shown in Table 1. For this study, the response was obtained through RTHS, as shown in Figure 2. RTHS is a method by which the real object is shaken if there are uncertainties in the modeling. The response is obtained by numerical simulation for other parts of the model. For this study, the MR damper was shaken using a shaking table. The measured damper force was added to solve the equations of motion of the building model to obtain the response continuously. For this experiment, the sampling frequency was set as 500 Hz. The input ground motion and magnification factor are presented in Table 2. The input magnification was set to the maximum magnification within the range of possible shaking table experiments. Here, $x(t)$, $\dot{x}(t)$, and,$\ddot{x}(t)$ respectively denote the response displacement, response velocity, and response acceleration of the superstructure.

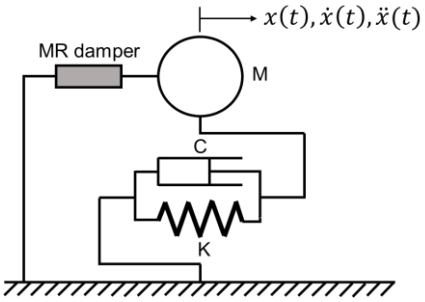

Figure 1. One-mass semi-active base-isolation system

Table 1. Model specifications

Mass (kg)	1.49×10^4
Stiffness (kN/m)	42.33
Damping factor (%)	3.58
Natural period (s)	3.72

Table 2. Input ground motion and magnification

input ground motion	El Centro 1940 NS	JR Takatori 1995 NS	Sylmar 1994 NS	Tomakomai 2003 NS	BCJ-L2
input magnification	100%	30%	40%	30%	40%

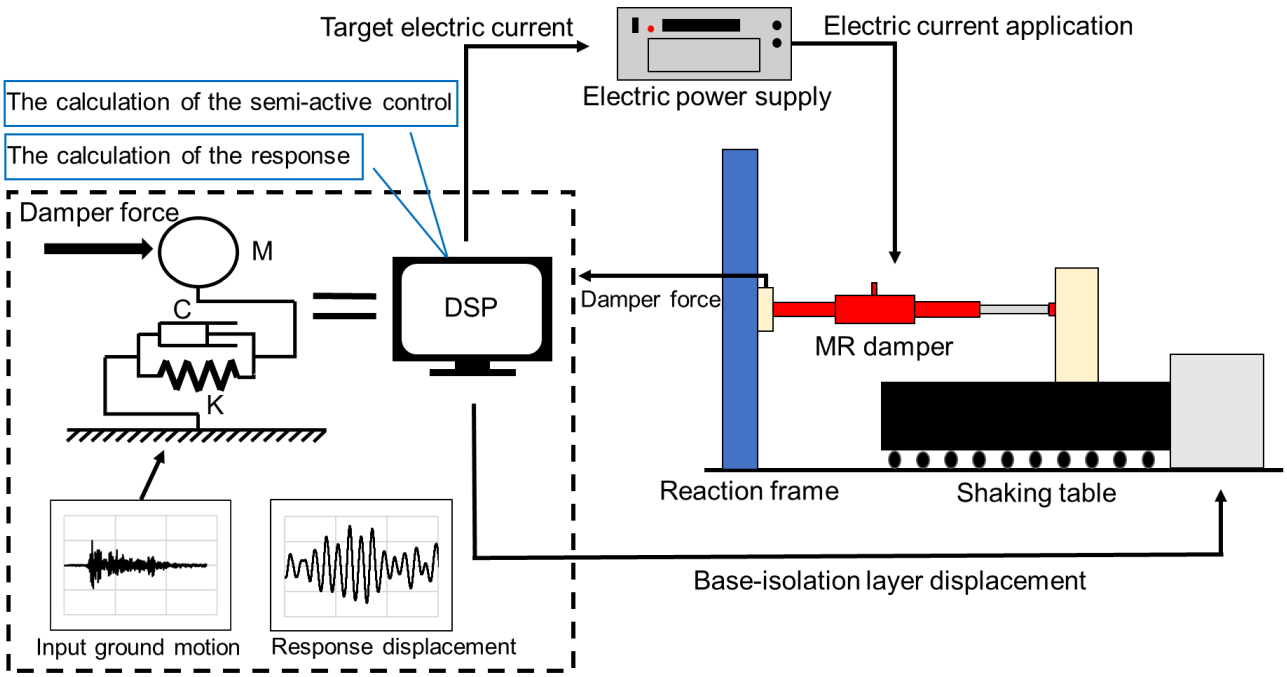

Figure 2. Schematic diagram of RTHS

2.2. Magnetorheological fluid damper (MR damper) (Itahara et al. (2020))

An MR damper (Figure 3), based on a conventional hydraulic damper mechanism, is filled with magneto-rheological fluid. The MR damper, a semi-active control device, obtains the desired damping force along the magnetic field acting on the MR fluid by varying the electric current applied to the electromagnets. For this study, the Bingham plastic model was used to model the MR damper as shown in Figure 4. The damper force of the MR damper F_{MR} is the sum of the variable Coulomb friction force and the viscous damping force proportional to the velocity, as shown in Equation (1). The MR damper_model used for this study was obtained from sinusoidal excitation experiments of the MR damper, as shown in Equation (2).

$$F_{MR} = F_c sgn(v) + Cv \text{ (kN)} \quad (1)$$

$$F_{MR} = (-0.219I^2 + 2.459I + 0.024)sgn(v) + (0.923I + 0.794)v \quad \text{(kN)} \quad (2)$$

F_{MR} : MR damper force (kN), F_c : variable Coulomb friction force (kN)
v : piston speed of MR damper (m/s), C: viscous damping coefficient (kN s/m)

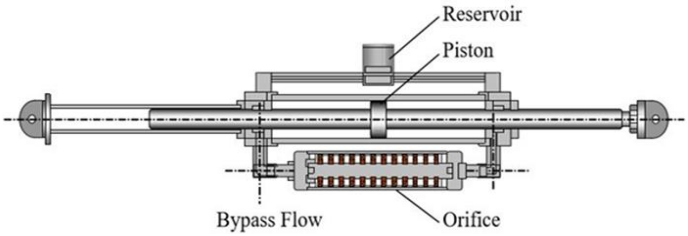

Figure 3. MR damper structure

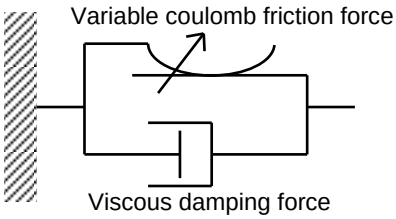

Figure 4. Bingham plastic model

2.3. Semi-active control

For this study, the semi-active control method shown in 2.3.1–2.3.3 was applied. As a comparison of semi-active control, velocity-proportional control values of 20% and 30% (designated as vp20% and vp30%, respectively) were used to provide damping force corresponding to damping factors of 20% and 30%.

2.3.1. Energy Function (EF) control (Shiozaki et al. (2003))

The EF control method calculates the required control force based on the vibration energy (sum of kinetic energy and elastic strain energy). The control force f_{EF} is obtained as shown in Equation (3). The gain λ is set to the square root of the vibration energy.

$$f_{EF} = \lambda \sqrt{\frac{1}{2}m\dot{x}^2 + \frac{1}{2}kx^2} \quad (3)$$

2.3.2. Linear Quadratic Regulator (LQR) control (Yang (1975))

The LQR control method determines the control force by minimizing the integral of the quadratic form of the relative displacement, relative velocity, absolute acceleration, and control input via the weights α, β, γ, and μ, as shown in Equation (4), which are the evaluation functions. Also, $\ddot{z}$ represents the ground acceleration.

$$J = \int_0^\infty (\alpha(\ddot{x} + \ddot{z})^2 + \beta\dot{x}^2 + \gamma x^2 + \mu u^2)dt \quad (4)$$

2.3.3. Sliding Mode Control (SMC) (Nonami et al. (1994))

An SMC control system consists of the reaching mode, which moves from an arbitrary position on a phase plane with displacement on the horizontal axis and velocity on the vertical axis to the switching plane, and the sliding mode, which converges to the origin by constraining the state on the switching plane after reaching the switching plane. The state space equation and the switching function are shown in Equation (5). Parameter S can be found using the pole assignment method.

$$\begin{cases} \dot{x} = Ax + Bu \\ \sigma(x) = Sx \end{cases} \tag{5}$$

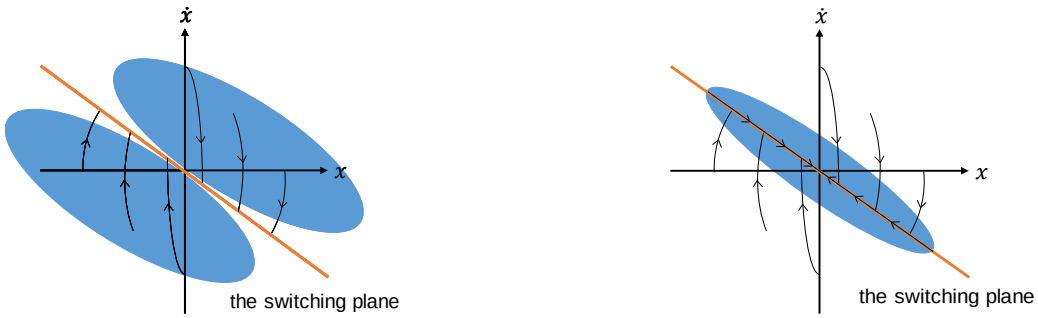

(a) Reaching mode *(b) Sliding mode*

Figure 5. Schematic diagram of Sliding Mode Control

3. RTHS results

Figures 6–10 show the experimentally obtained results of (a) the relation of maximum relative displacement – maximum absolute acceleration and (b) the relation of maximum relative displacement – absolute acceleration RMS values. Those figures show that semi-active control is more effective than passive control for reducing the relative displacement and absolute acceleration, except for some near-fault pulse ground motion. Particularly, LQR reduced the maximum relative displacement the most. Also, SMC was able to reduce both the relative displacement and absolute acceleration considerably.

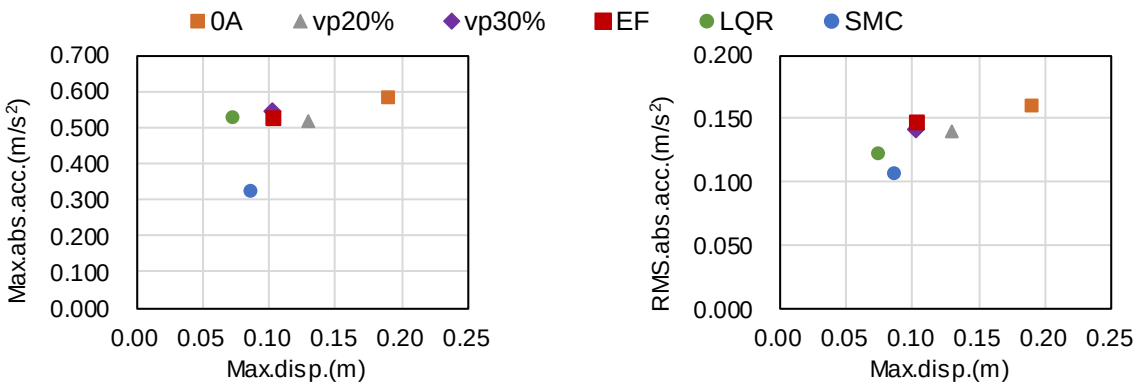

(a) Max. disp. – Max. abs. acc. *(b) Max. disp. – RMS. abs. acc.*

Figure 6. RTHS results obtained under El Centro 1940 NS

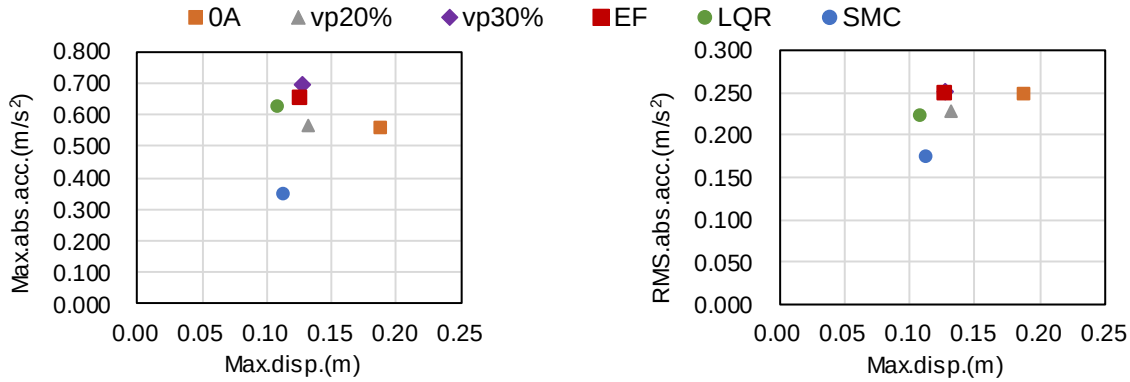

(a) Max. disp. – Max. abs. acc. *(b) Max. disp. – RMS. abs. acc.*

Figure 7. RTHS results obtained under JR Takatori 1995 NS

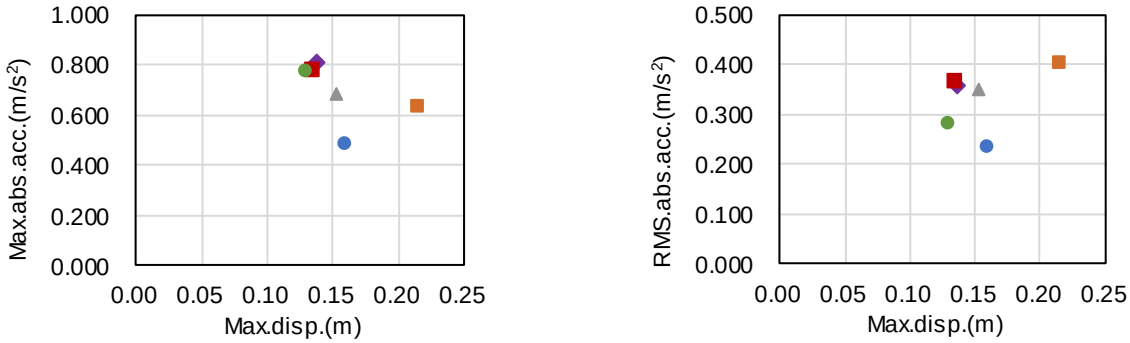

(a) Max. disp. – Max. abs. acc. *(b) Max. disp. – RMS. abs. acc.*

Figure 8. RTHS results obtained under Sylmar 1994 NS

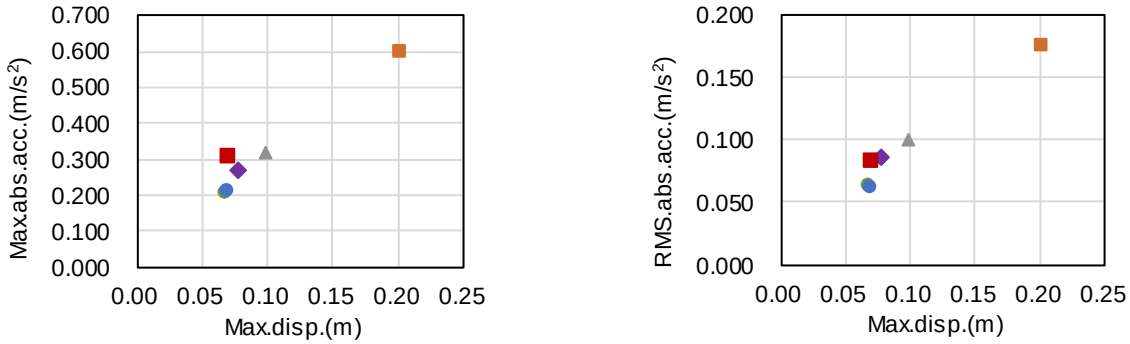

(a) Max. disp. – Max. abs. acc. *(b) Max. disp. – RMS. abs. acc.*

Figure 9. RTHS results obtained under Tomakomai 2003 NS

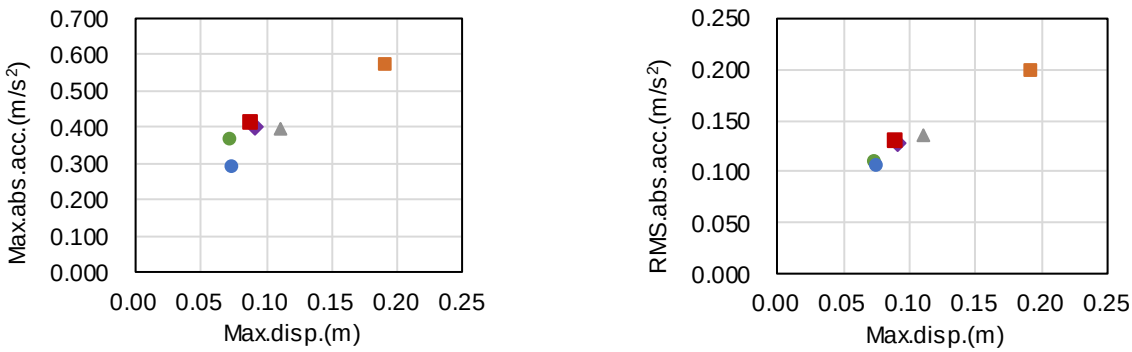

(a) Max. disp. – Max. abs. acc. *(b) Max. disp. – RMS. abs. acc.*

Figure 10. RTHS results obtained under BCJ-L2

4. Identification by ARX model

4.1. One-input, one-output ARX model (Saito (1998))

The ARX model, a time-domain system identification method, is used to identify the damping factor for each control. For this study, a one-input, one-output ARX model is used to identify the natural frequency and the damping factor of the single-degree-of-freedom system. The model input is the ground acceleration; the model output is the absolute acceleration of the superstructure.

With output $y(t)$, input $u(t)$, and white noise $e(t)$ with mean zero, the one-input, one-output ARX model is represented by Equation (6). Therein, $A(q)$ and $B(q)$ are polynomials of the time delay operator q^{-1}, as in Equations (7) and (8). Also, n_k is the delay time. The identified natural frequencies are represented by f_j in Equation (9) and the damping constants by h_j in Equation (10). Therein, ${}_zp_j$ is the root of $A(z) = 0$ when $A(z)$ is the discrete-time representation of $A(q)$; Δt is the sampling time. For this study, the ARX model from Matlab's System Identification Toolbox was used.

$$A(q)y(t) = B(q)u(t) + e(t) \tag{6}$$

$$A(q) = 1 + \sum_{j=1}^{na} a_j q^{-j} \tag{7}$$

$$B(q) = \sum_{j=1}^{nb} b_j q^{-j+1-n_k} \tag{8}$$

$$f_j = \frac{|\log_e {}_zp_j|}{2\pi\Delta t} \tag{9}$$

$$h_j = \frac{-\log_e|{}_zp_j|}{2\pi f_j \Delta t} \tag{10}$$

4.2. Identification Results

A bandpass filter was applied to both the input ground acceleration and the absolute acceleration of the superstructure obtained in the RTHS to identify the natural frequencies and the damping factor using the ARX model. The range of the bandpass filter was 0.1–0.5 Hz, which includes the frequency of the peak of the experimental transfer function. Because data with small responses might reflect large experiment errors, the ARX model was applied using data from time durations when large response values were generated. The data duration time and sampling frequency were set respectively as 35 s and 10 Hz.

Table 3 shows the identification results. The no-current, velocity-proportional, and EF controls identified values close to the natural frequencies of the one-mass model for all ground motions, whereas the LQR and SMC controls tended to identify smaller natural frequencies than those of the other controls. A comparably larger damping factor was obtained for LQR and SMC than for the other controls. Particularly for LQR control, the largest damping factors were obtained for all ground motions.

Table 3 Identification results

(a) El Centro 1940 NS

	0A	vp20%	vp30%	EF	LQR	SMC
Natural frequency	0.2739	0.2718	0.2780	0.2760	0.1729	0.1397
Damping factor	0.0885	0.2283	0.3380	0.3307	0.6776	0.6569

(b) JR Takatori 1995 NS

	0A	vp20%	vp30%	EF	LQR	SMC
Natural frequency	0.2699	0.2738	0.2722	0.2755	0.1693	0.1883
Damping factor	0.0745	0.2386	0.3463	0.3161	0.6434	0.4684

(c) Sylmar 1994 NS

	0A	vp20%	vp30%	EF	LQR	SMC
Natural frequency	0.2703	0.2758	0.2685	0.2729	0.1161	0.1930
Damping factor	0.0772	0.2329	0.3143	0.3331	0.9100	0.5906

(d) Tomakomai 2003 NS

	0A	vp20%	vp30%	EF	LQR	SMC
Natural frequency	0.2688	0.2733	0.2786	0.2725	0.2444	0.2379
Damping factor	0.0769	0.2316	0.3205	0.3907	0.6123	0.6017

(e) BCJ-L2

	0A	vp20%	vp30%	EF	LQR	SMC
Natural frequency	0.2714	0.2726	0.2753	0.2746	0.1577	0.1535
Damping factor	0.0839	0.2330	0.3419	0.3383	0.7815	0.7423

4.3. Correspondence between identified damping factor and RTHS results

Figures 11–15 show the correspondence between the identified damping factor and RTHS results of (a) maximum relative displacement, (b) maximum absolute acceleration, and (c) absolute acceleration RMS values at El Centro 1940 NS, JR Takatori 1995 NS, Sylmar 1994 NS, Tomakomai 2003 NS, and BCJ-L2 inputs.

The magnitude relation of the damping factor identified by the ARX model corresponds to the magnitude relation of the reduction effect of the maximum relative displacement, but not to the magnitude relation of the reduction effect of the absolute acceleration in the case of LQR, where the response reduction is large. Particularly for JR Takatori 1995 NS and Sylmar 1994 NS, which are near-fault seismic motions, the magnitude relation of the identified damping factors does not correspond to the magnitude relation of the absolute acceleration reduction effect.

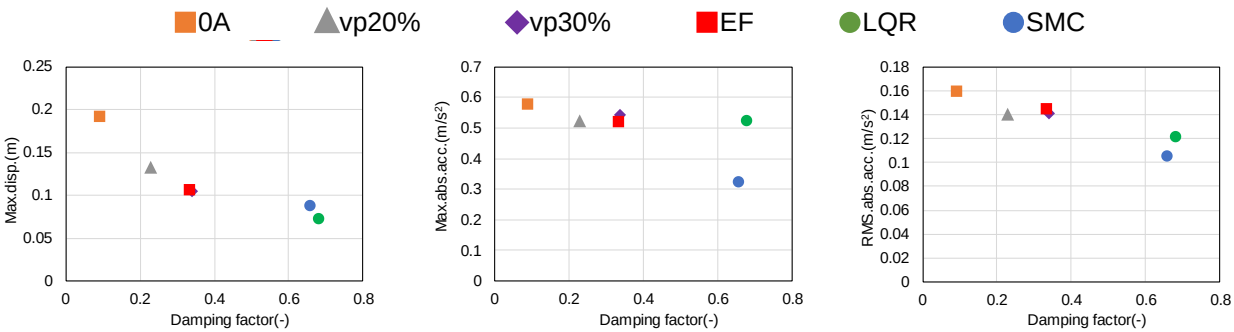

(a) Damping factor – Max. disp. *(b) Damping factor – Max. abs. acc.* *(c) Damping factor – RMS. abs. acc.*

Figure 11. El Centro 1940 NS

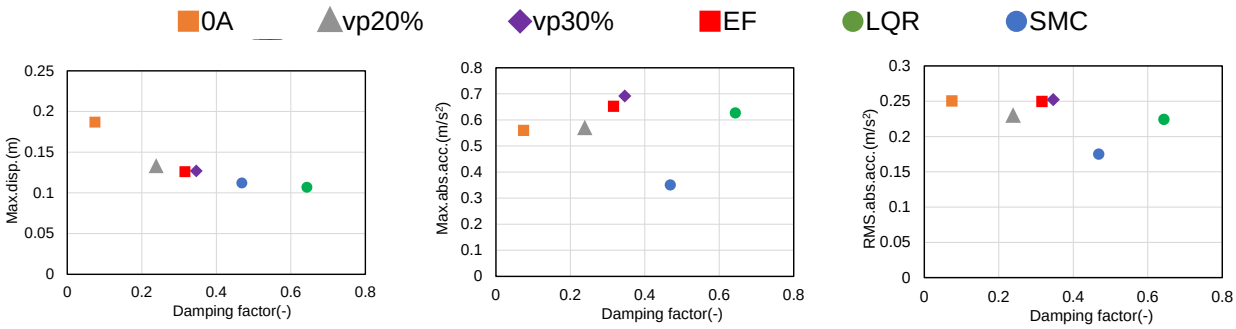

(a) Damping factor – Max. disp. *(b) Damping factor – Max. abs. acc.* *(c) Damping factor – RMS. abs. acc.*

Figure 12. JR Takatori 1995 NS

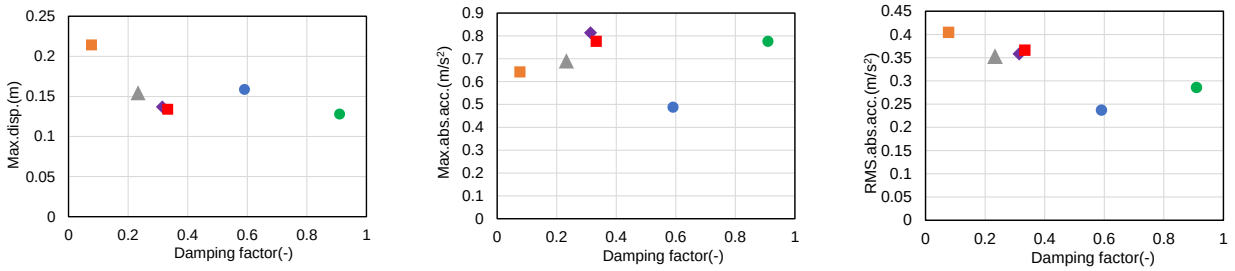

(a) Damping factor – Max. disp. *(b) Damping factor – Max. abs. acc.* *(c) Damping factor – RMS. abs. acc.*

Figure 13. Sylmar 1994 NS

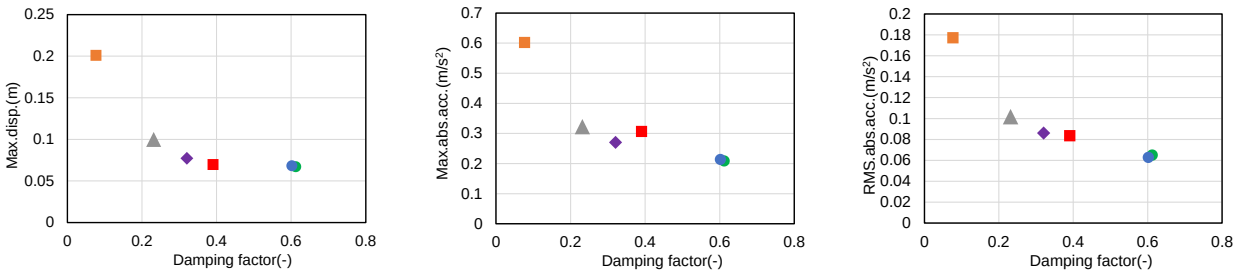

(a) Damping factor – Max. disp. *(b) Damping factor – Max. abs. acc.* *(c) Damping factor – RMS. abs. acc.*

Figure 14. Tomakomai 2003 NS

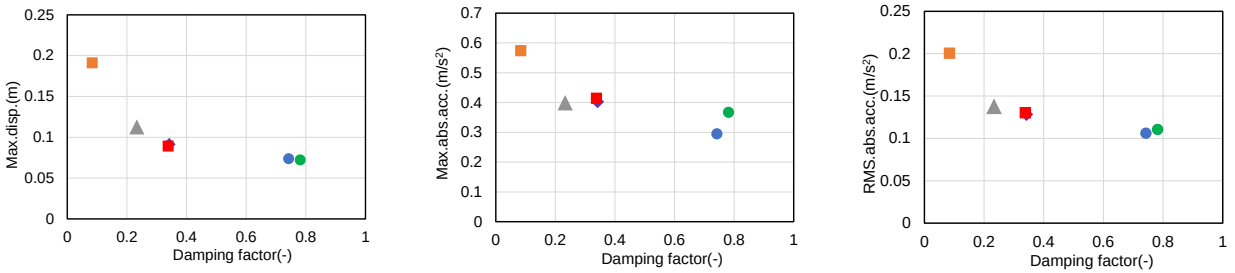

(a) Damping factor – Max. disp. *(b) Damping factor – Max. abs. acc.* *(c) Damping factor – RMS. abs. acc.*

Figure 15. BCJ-L2

4.4. Comparison of identified and approximated damping factor

The approximate damping factor is obtained from the velocity–damper force relation of the MR damper (Figure 16) and compared with the results of identifying the damping factor using the ARX model. The velocity–damper force relation of the MR damper is approximated as a linear function, the slope of which is the damping coefficient c_{MR} (kN s/m). The approximate damping factor h_{MR} of the MR damper is obtained using Equation (11). The sum of the obtained h_{MR} and the damping factor h_0 of the mass model, h', is used

as the approximate damping factor, as shown in Equation (12). Figure 17 presents a comparison of the damping factor obtained from the identification results and those obtained approximately. For passive control and EF control, the two values are close. By contrast, for LQR and SMC, the damping factors identified by the ARX model are larger for all ground motions.

$$h_{MR} = \frac{c_{MR}}{2\sqrt{mk}} \tag{11}$$

$$h' = h_{MR} + h_0 \tag{12}$$

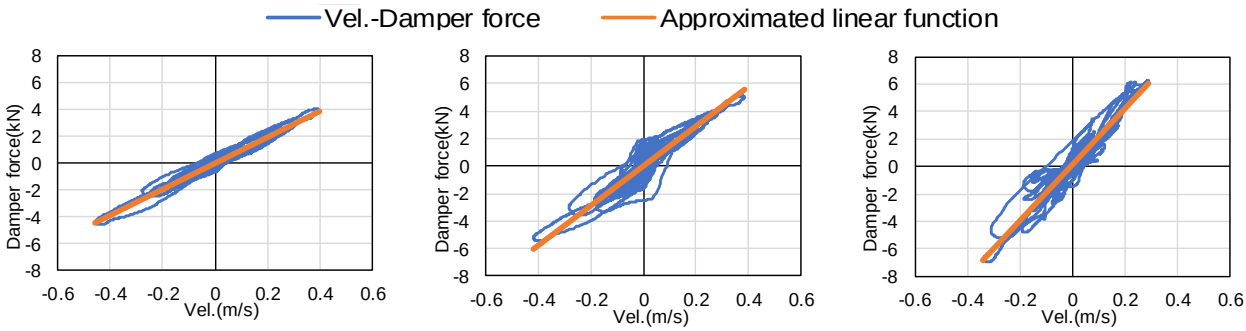

(a) vp20% *(b) EF* *(c) LQR*

Figure 16. Vel.-Damper force and Approximated linear function

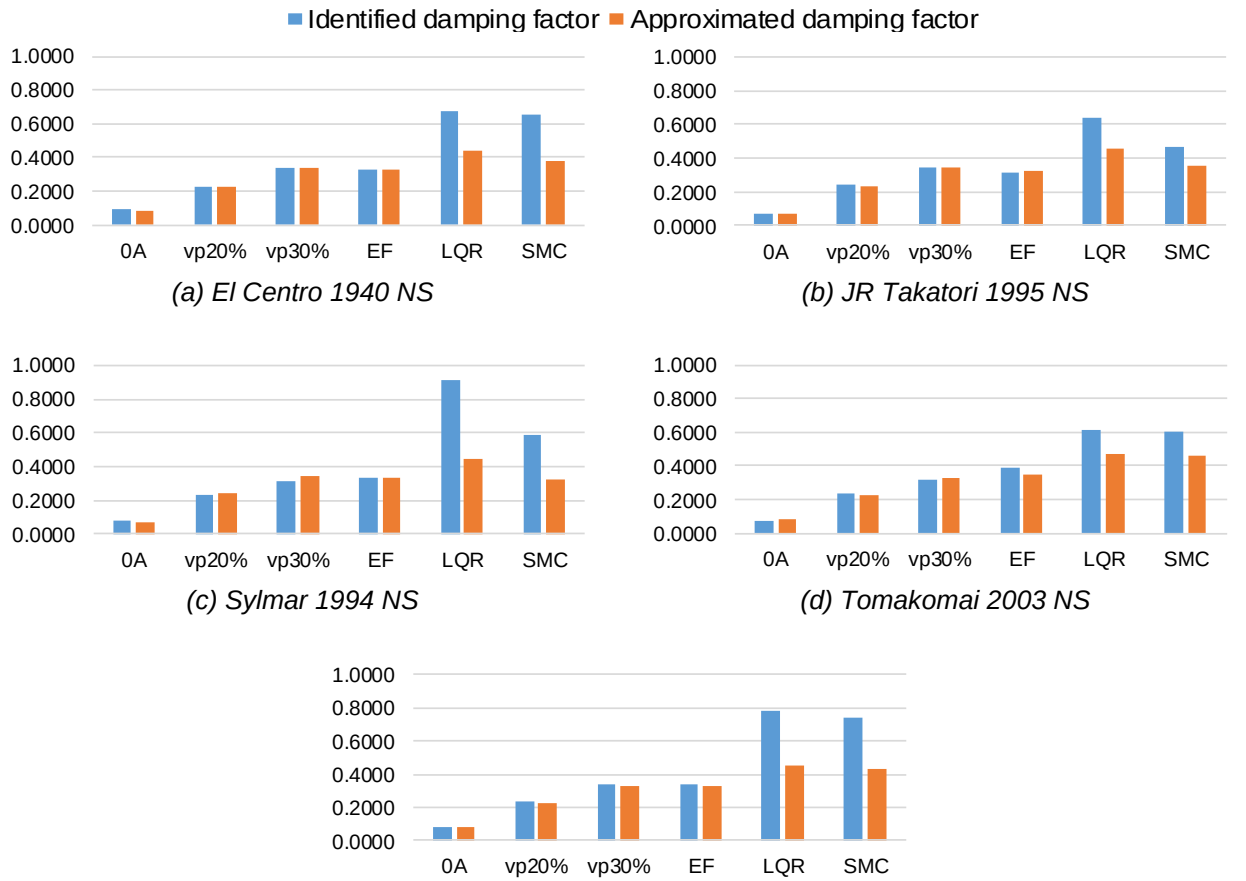

(a) El Centro 1940 NS *(b) JR Takatori 1995 NS*

(c) Sylmar 1994 NS *(d) Tomakomai 2003 NS*

(e) BCJ-L2

Figure 17. Damping factors

4.5. Simulation using identification results

Simulation of the single-degree-of-freedom system was conducted given the natural frequency and damping factors obtained from the identification results. The findings were compared with the RTHS results. Figure 18 compares the absolute accelerations for the El Centro 1940 NS 100% input. For all control methods, the absolute accelerations from the RTHS and the numerical simulation generally mutually agreed. The ARX model was able to identify the natural frequency and damping factor with good accuracy.

Tables 4–8 present comparison of the maximum relative displacement, maximum absolute acceleration, and RMS values of absolute acceleration for the RTHS and analytical values. For passive control and EF control, the RTHS and analytical values are mutually close, suggesting that they were identified with good accuracy. For LQR and SMC, the maximum absolute acceleration values differ between the experimentally obtained and analytically obtained values, but the maximum relative displacement and absolute acceleration RMS values are approximately equal, indicating that they were identified with good accuracy, except for LQR under JR Takatori 1995 NS and Sylmar 1994 NS.

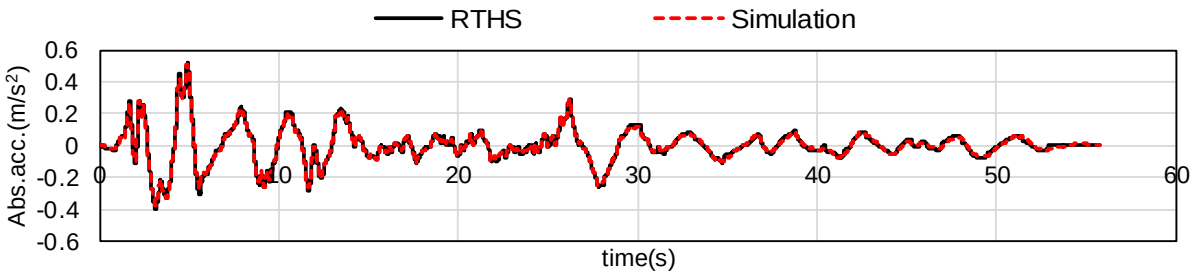

(a) vp20%

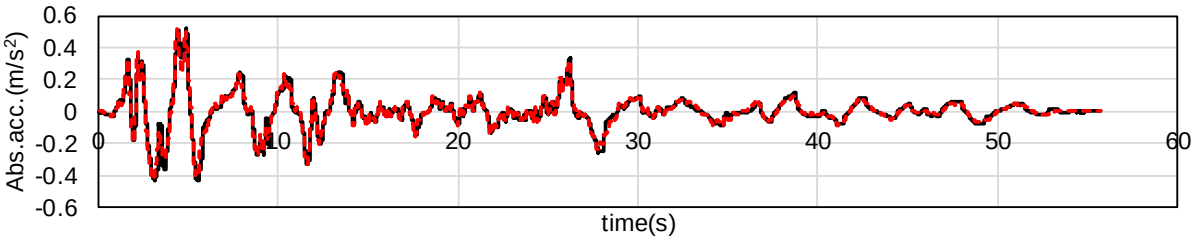

(b) EF

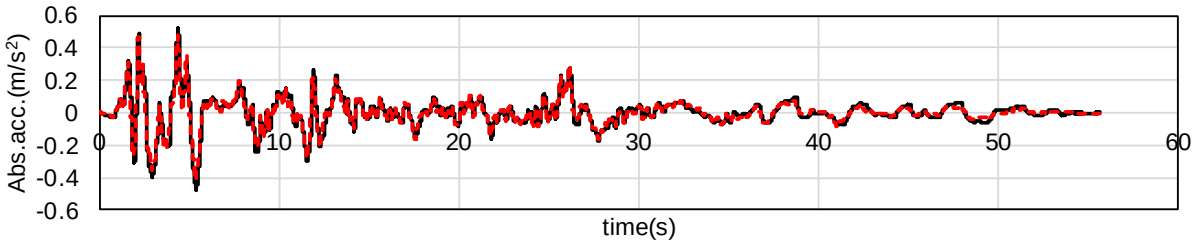

(c) LQR

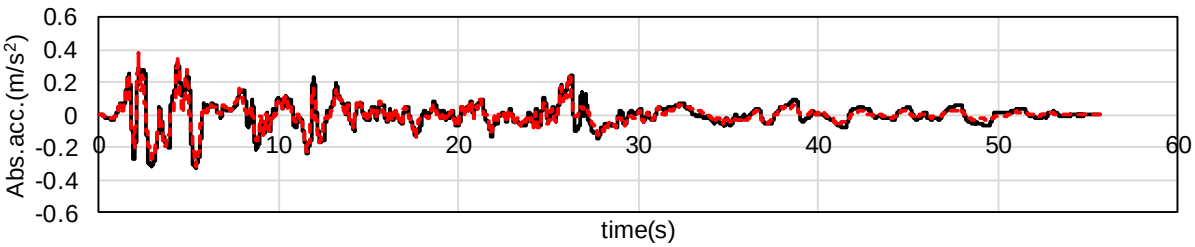

(d) SMC

Figure 18. Absolute accelerations found using RTHS and simulations (El Centro 1940 NS)

Table 4. Response values obtained for El Centro 1940 NS

(a) RTHS (b) Simulation

	0A		vp20%		vp30%		EF		LQR		SMC	
	(a)	(b)	(a)	(b)	(a)	(b)	(a)	(b)	(a)	(b)	(a)	(b)
Max. disp. (m)	0.1925	0.1837	0.1313	0.1311	0.1043	0.1049	0.1063	0.1064	0.0735	0.0752	0.0877	0.0808
Max. abs. acc. (m/s^2)	0.5799	0.5782	0.5169	0.5149	0.5431	0.5371	0.5226	0.5217	0.5254	0.4733	0.3241	0.3750
RMS. abs. acc. (m/s^2)	0.1609	0.1652	0.1401	0.1354	0.1420	0.1394	0.1458	0.1377	0.1229	0.1087	0.1058	0.0863

Table 5. Response values obtained for JR Takatori 1995 NS

(a) RTHS (b) Simulation

	0A		vp20%		vp30%		EF		LQR		SMC	
	(a)	(b)	(a)	(b)	(a)	(b)	(a)	(b)	(a)	(b)	(a)	(b)
Max. disp. (m)	0.1895	0.1871	0.1339	0.1314	0.1287	0.1234	0.1285	0.1258	0.1072	0.1007	0.1136	0.1095
Max. abs. acc. (m/s^2)	0.5590	0.5509	0.5656	0.5426	0.6912	0.6497	0.6518	0.6308	0.6262	0.5397	0.3508	0.4820
RMS. abs. acc. (m/s^2)	0.2504	0.2506	0.2286	0.2215	0.2523	0.2370	0.2497	0.2351	0.2242	0.1869	0.1751	0.1675

Table 6. Response values obtained for Sylmar 1994 NS

(a) RTHS (b) Simulation

	0A		vp20%		vp30%		EF		LQR		SMC	
	(a)	(b)	(a)	(b)	(a)	(b)	(a)	(b)	(a)	(b)	(a)	(b)
Max. disp.(m)	0.2158	0.2053	0.1552	0.1540	0.1383	0.1355	0.1457	0.1336	0.1279	0.1281	0.1599	0.1247
Max. abs. acc. (m/s^2)	0.6419	0.6055	0.6847	0.6611	0.8137	0.7275	0.7762	0.7613	0.7757	0.6264	0.4883	0.7323
RMS. abs. acc. (m/s^2)	0.4045	0.3955	0.3504	0.3489	0.3584	0.3254	0.3661	0.3352	0.2857	0.2052	0.2371	0.2515

Table 7. Response values obtained for Tomakomai 2003 NS

(a) RTHS (b) Simulation

	0A		vp20%		vp30%		EF		LQR		SMC	
	(a)	(b)	(a)	(b)	(a)	(b)	(a)	(b)	(a)	(b)	(a)	(b)
Max. disp. (m)	0.2024	0.2034	0.0991	0.0960	0.0777	0.0742	0.0707	0.0655	0.0675	0.0508	0.0687	0.0532
Max. abs. acc. (m/s^2)	0.6020	0.5869	0.3185	0.3069	0.2707	0.2662	0.3068	0.2428	0.2085	0.2121	0.2137	0.2061
RMS. abs. acc. (m/s^2)	0.1771	0.1853	0.1005	0.0981	0.0861	0.0839	0.0834	0.0761	0.0650	0.0630	0.0629	0.0624

Table 8. Response values obtained for BCJ-L2

(a) RTHS (b) Simulation

	0A		vp20%		vp30%		EF		LQR		SMC	
	(a)	(b)	(a)	(b)	(a)	(b)	(a)	(b)	(a)	(b)	(a)	(b)
Max. disp. (m)	0.1928	0.1847	0.1119	0.1109	0.0919	0.0902	0.0904	0.0909	0.0727	0.0833	0.0744	0.0889
Max. abs. acc. (m/s^2)	0.5745	0.5570	0.3946	0.3933	0.4029	0.3874	0.4144	0.3847	0.3667	0.2903	0.2950	0.2740
RMS. abs. acc. (m/s^2)	0.2004	0.2016	0.1362	0.1339	0.1283	0.1252	0.1302	0.1250	0.1105	0.0921	0.1062	0.0877

5. Conclusion

1. The RTHS confirmed that semi-active control can better reduce the base-isolation layer's response displacement without amplifying the superstructure's response acceleration compared to the response with no electric current applied.
2. The magnitude relation of the damping factor identified using the ARX model corresponds to the magnitude relation of the reduction effect of the maximum relative displacement, but not to the magnitude relation of the reduction effect of the absolute acceleration in the case of LQR, for which the response reduction is large.
3. In cases where the control force has strong linearity with the damping force, such as passive control and EF control, the damping factor obtained from the identification results and the approximate damping factor obtained from the velocity-damper force relation were close for all ground motions.
4. Comparison of the analytical and RTHS results of the single-degree-freedom-system given the natural frequency and damping factor obtained from the identification results shows that the maximum relative displacement, maximum absolute acceleration, and absolute acceleration RMS values for passive control and EF control are all nearly equal those of the experiment and simulation, indicating that the ARX model is useful for accurate identification. For LQR and SMC, the maximum relative displacement values were also close. Generally accurate identification was achieved.

Acknowledgments

This work was supported by JSPS KAKENHI Grant Number JP22H01643.

References

Johnson, E.A., Ramallo, J. C., Spencer Jr., B. F. and Sain, M. K. (1998). Intelligent Base Isolation Systems, *Proceedings of the Second World Conference on Structural Control*, Kyoto, Japan: 367–376.

Fujii H., Hiwatashi T., Fujitani H. (2007). SHAKING TABLE TEST OF SEMI−ACTIVE CONTROL FOR BASE−ISOLATION SYSTEM BY MR-DAMPER APPLIED WITH OPTIMAL REGULATOR THEORY - Effect of changing weighting matrix -, *Journal of Structural and Construction Engineering*, Vol.72, No.618: 73–79. (in Japanese)

Itahara K., Fujitani H., Mukai Y., Ito M., Sato E., Iba S. (2020). SHAKING TABLE TEST AND REAL-TIME HYBRID SIMULATION IN SEMI-ACTIVE CONTROLLED BASE-ISOLATION SYSTEM, *Proceedings of the 17th World Conference on Earthquake Engineering (17WCEE)*, Paper No. 2g-0136, Sendai, Japan.

Shiozaki Y., Hiwatashi T., Fujitani H., Soda S. (2003). SIMPLE SEMI−ACTIVE CONTROL FOR BASE−ISOLATED BUILDING BY MR DAMPER, *Journal of Structural and Construction Engineering*, Vol.68, No.570: 37–43. (in Japanese)

Yang, J. N. (1975). Application of Optimal Control Theory to Civil Engineering Structures, *Journal of The Engineering Mechanics Division*, Vol.101, No.6: 819–838.

Nonami K., Tian. H. (1994). Sliding Mode Control - Theory of non-linear robust control design -, Corona Publishing Co., Tokyo Japan, (in Japanese)

Saito T. (1998). SYSTEM IDENTIFICATION OF A HIGH−RISE BUILDING APPLYING MULTI-INPUT−MULTI-OUTPUT ARX MODEL OF MODAL ANALYSIS, *Journal of Structural and Construction Engineering*, Vol.63, No.508: 47–54. (in Japanese)